CHEMISTRY
A EUROPEAN JOURNAL

FULL PAPER

DOI: 10.1002/chem.201201471

Dynamically Controllable Emission of Polymer Nanofibers: Electrofluorescence Chromism and Polarized Emission of Polycarbazole Derivatives

Kohsuke Kawabata and Hiromasa Goto*[a]

Abstract: Electrochemical polymerization of a series of *N*-alkyl-2,7-di(2-thienyl)carbazoles in acetonitrile was performed to obtain conjugated polymers with fluorescence. Scanning electron and atomic force microscopies revealed that the surface morphology of the polymer films significantly depends on the alkyl chain lengths of the polymers. Particularly, a homopolymer bearing hexyl groups and copolymers with an average alkyl chain length of six carbon atoms show nanofiber morphology. The polymer nanofibers were stacked on a substrate electrode. The fluorescence of the polymer nanofiber film was tunable with application of voltage, with good repeatability. The X-ray diffraction pattern of the fibers showed the structural order. The polymer nanofibers thus prepared showed an electrochemically driven change in polarized photoluminescence.

Keywords: electrochemistry · electrochromism · luminescence · nanostructures · polymerization

Introduction

Photoluminescence (PL) and electroluminescence are light-emitting processes occurring through relaxation of excited electrons, which can be widely observed not only in synthetic dyes,[1] but also in living creatures and plants, especially in deep-sea fish,[2] since surprisingly some species can control the emission of light.

π-Conjugated polymers showing PL and electroluminescence have been developed for application in light-emitting devices[3,4] and as photosensing materials.[5,6] Among many synthetic methods for obtaining conjugated polymers, electrochemical polymerization is a useful method for the preparation of electroactive polymeric thin films. The electrochemical process is a noncatalytic reaction, and the polymerization method provides good reproducibility because the polymerization process can be easily controlled by monitoring the current and integrated charge passed through electrochemical cells. Monomers for electrochemical polymerization require no modification of chemical structure to obtain reactive sites, such as −Cl, −Br, −I, $-SnR_3$, and $-B(OR)_2$. Furthermore, the electrochemical method requires no cumbersome purification process.

Generally, electron-rich heteroaromatic rings, such as pyrrole, furan, thiophene, and 3,4-ethylenedioxythiophene, which have relatively low oxidation potentials, are introduced in structures of monomers for electrochemical polymerization[7–10] because the initial step of electrochemical polymerization is oxidation of monomers.[11,12] The monomers with low oxidation potential can be polymerized to produce low-bandgap polymers. To date, many kinds of electrochemically synthesized polymers have been reported for various applications, such as electrochromic devices,[13,14] organic light-emitting diodes,[15–17] and organic photovoltaics.[18–20] Electrochemical polymerization produces conjugated polymer films with various surface structures and morphologies, which depend on the monomer structures and polymerization conditions.[21–23] Surface structure and morphology strongly influence the properties of polymeric materials. To control the surface structure and morphology of electrochemically synthesized polymers, many techniques have been developed, which can produce nanoarrays,[24] nanotubes,[25] nanospheres,[26] nanocapsules,[26] and nanofibers.[27] Such nanostructured conjugated polymers, especially nanofibers, have attracted much attention for their functionality in application to optoelectrics.[28–33]

Herein, we demonstrate electrochemical polymerization and copolymerization of a series of *N*-alkyl-2,7-di(2-thienyl)carbazoles (TCz*m*; alkyl chain length $m=2$–8) in acetonitrile. The surface morphology of the polymers, observed with scanning electron microscopy (SEM), depends on the alkyl chain length. For the polymer with a hexyl group, nanofiber formation is observed; these fibers exhibit fluorescence and show an electrochemically driven PL switching function. Furthermore, the crystallinity and polarized emission of the polymer nanofiber film are examined.

[a] K. Kawabata, Prof. H. Goto
Faculty of Pure and Applied Sciences
University of Tsukuba
Tsukuba, Ibaraki 305-8573 (Japan)
Fax: (+81) 29-8534490
E-mail: gotoh@ims.tsukuba.ac.jp

Supporting information for this article is available on the WWW under http://dx.doi.org/10.1002/chem.201201471.

Results and Discussion

An electrochemical oxidative coupling reaction between TCz*m* molecules afforded α-position linkage between thiophene rings, to give the corresponding conjugated polymers and random copolymers (PTCz*m* and PTCz(*k*-*l*), respectively), as shown in Scheme 1.

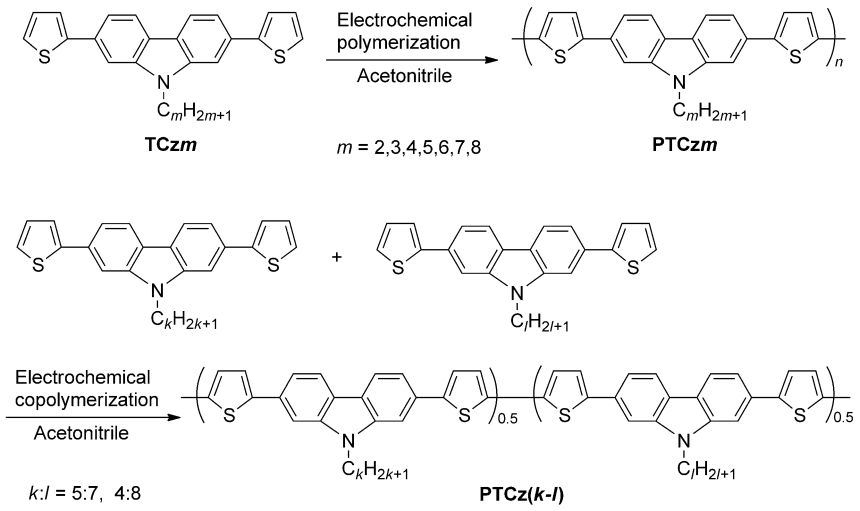

Scheme 1. Electrochemical polymerization and copolymerization of TCz*m*.

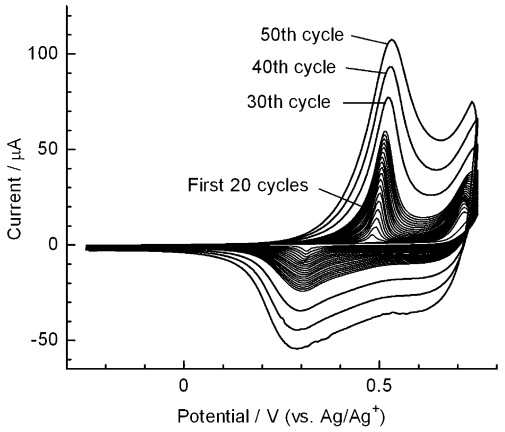

Figure 1. Cyclic voltammograms for electrochemical polymerization of TCz6 obtained by using a platinum disk working electrode, a platinum wire counter electrode, and an Ag/Ag^+ reference electrode. The electrolyte solution contained 0.1 M tetrabutylammonium perchlorate and 1.0 mM TCz6 in acetonitrile. The scan rate was 100 mV s^{-1}.

Figure 1 shows cyclic voltammograms for the electrochemical polymerization of TCz6 by using a platinum disk working electrode. The oxidation current onset of the first cycle corresponded to the oxidation potential of TCz6 of 0.67 V (vs. Ag/Ag^+; the other monomers show the same oxidation potential). Oxidation potentials of related molecules were evaluated experimentally in a previous report,[34] and reported theoretically with DFT calculations.[35] An increase in the current response intensity in sequential cycles indicated the progress of the polymerization reaction. Oxidation and reduction current signals at about 0.5 and 0.3 V, respectively, corresponded to oxidation and reduction of a π-conjugated system of the resulting polymer deposited on the electrode. Lowering of the oxidation and reduction current onsets with an increase in number of cycles indicated extension of effective conjugation length in the polymer backbone. The growth of the conjugated polymer chains is also confirmed by in situ UV/Vis absorption spectroscopy during electrochemical polymerization of TCz6 (Figure S1 in the Supporting Information).

The infrared (IR) absorption spectrum of PTCz6 in the neutral state shows absorption bands similar to those of the monomer (TCz6), although the bands are slightly broadened (Figure S2 in the Supporting Information). However, an absorption band of TCz6 at 806 cm^{-1} due to the C–H bending vibration (δ_{C-H}) of the thiophene unit was shifted to 792 cm^{-1} after electrochemical polymerization. This band at 792 cm^{-1} is characteristic of the C–H bending vibration (δ_{C-H}) of 2,5-substituted thiophenes.[36,37] Therefore, the energy shift indicated the occurrence of a coupling reaction between monomers at α positions of thiophene units during electrochemical polymerization. Furthermore, an absorption band of TCz6 at 3100 cm^{-1}, which is characteristic of the α-position C–H stretching vibration of a thiophene ring, disappeared after polymerization, whereas an absorption band of TCz6 at 3070 cm^{-1}, due to the β-position C–H stretching vibration (ν_{C-H}) of thiophene, remained after the polymerization with a slight redshift of 5 cm^{-1}. This confirms that electrochemical polymerization of TCz6 afforded PTCz6 through a coupling reaction between α positions of thiophene units of TCz6.

The PTCz*m* films were insoluble in acetonitrile and acetone, and partially soluble in tetrahydrofuran and chloroform. Therefore, the molecular weights of the polymer films were not measurable with gel permeation chromatography. We examined the molecular weight of the polymer films by MALDI-TOF mass spectrometry (MS). Figure 2 shows MALDI-TOF mass spectra of PTCz6, PTCz(5-7), and PTCz(4-8). The MALDI-TOF mass spectrum of PTCz6 shows a certain pattern with a periodicity of 413 of *m*/*z*, which corresponds to the molecular weight of the monomer unit (413.13). In the measurements, peaks up to *m*/*z* 5375, which corresponds to 13-mers, were detected. The other homopolymers also show periodic patterns due to molecular

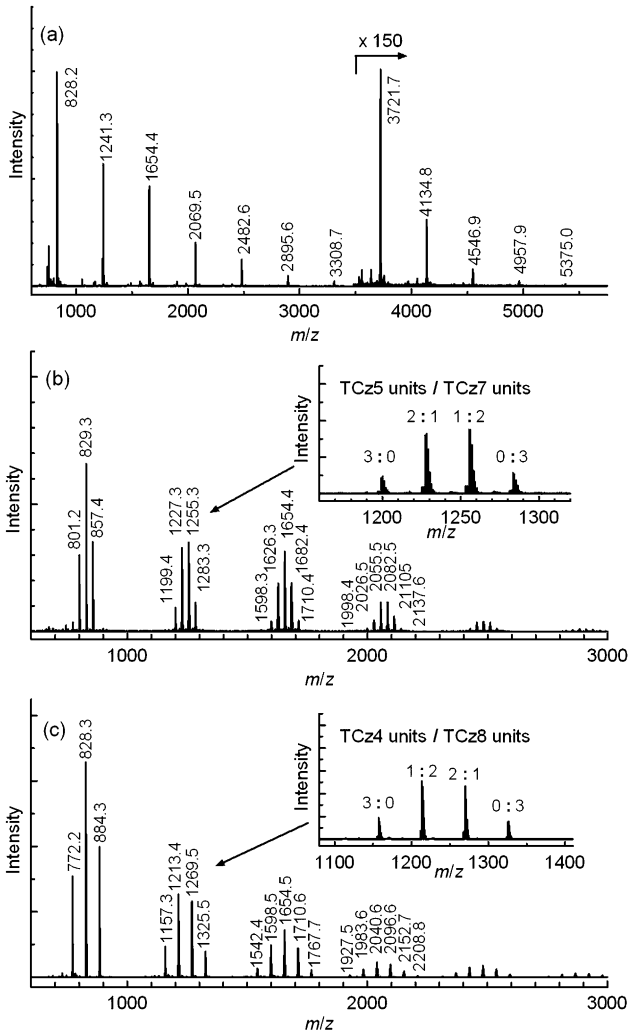

Figure 2. MALDI-TOF mass spectra of a) PTCz6, b) PTCz(5-7), and c) PTCz(4-8). Insets are magnifications of the spectra.

distribution of the monomer units (Figure S3 in the Supporting Information). The peak intensity of the spectra decreased with an increase in the m/z value. This result indicates that the MALDI-TOF MS measurements for the electrosynthesized polymer can evaluate the molecular weights of the low-molecular-weight fraction of the polymers. On the other hand, MALDI-TOF mass spectra of the copolymers PTCz(5-7) and PTCz(4-8) show periodic patterns with two types of periodicity. A long periodicity corresponds to an average molecular weight of two kinds of monomer units. For example, in the case of PTCz(5-7), the average molecular weight of two monomer units of TCz5 (=399.1) and TCz7 (=427.1) is 413.1, which is the same value as that of TCz6. A short periodicity corresponds to differences of molecular weights between two monomer units (28.0 for PTCz(5-7) and 56.1 for PTCz(4-8)). The periodic patterns with the short periodicity show symmetric distribution, which indicates that the two monomers have the same reactivity under these electrochemical random copolymerization conditions, and are introduced equally into the resulting copolymers.

The surface morphology of the polymer films electrodeposited on indium tin oxide (ITO) glass electrodes was observed with SEM. Generally, electrochemically polymerized polymer films have flat, porous, rugged, globular or cauliflower-like surface morphology. Figure 3 shows SEM images

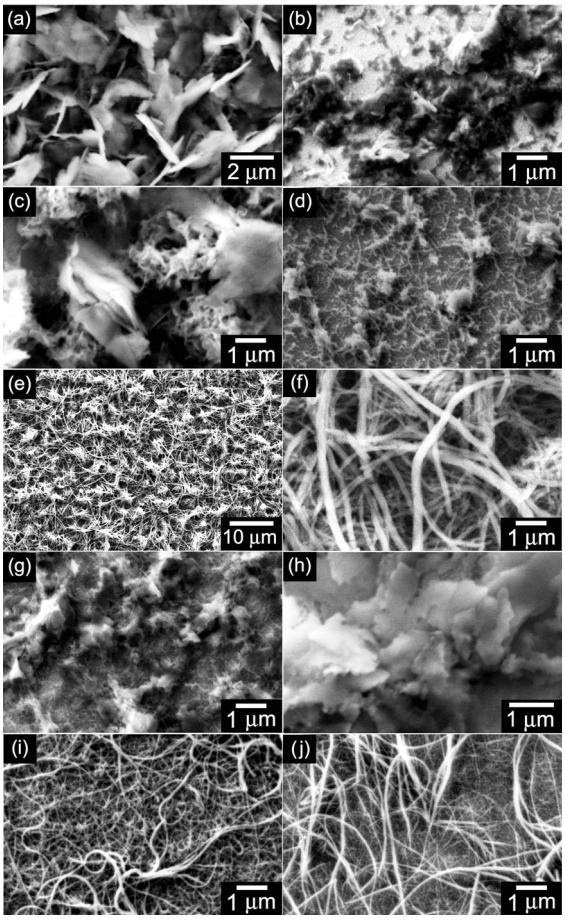

Figure 3. SEM images of surfaces of a) PTCz2, b) PTCz3, c) PTCz4, d) PTCz5, e) and f) PTCz6, g) PTCz7, h) PTCz8, i) PTCz(5-7), and j) PTCz(4-8) films electrodeposited on ITO glass electrodes.

of the polymer films. The surface morphology of the polymer films significantly depends on the alkyl chain length. PTCz2, 4, and 8 show some platelike structures, whereas PTCz5 and 7 show cauliflower-like structures with fine fiber structures. On the other hand, PTCz6 shows an entangled nanofiber structure (Figure 3e and f). The nanofibers have diameters of 100–200 nm and lengths of approximately 10 μm. The nanofibers stack on the substrate to form a film. The PTCz6 nanofiber film is insoluble in acetonitrile, but the entangled nanofibers are, to some extent, untangled with sonification in acetonitrile. Figure 4a and c show atomic force microscopy (AFM) images of untangled nanofibers on a glass substrate and their 3D profile, respectively. Figure 4b shows a cross-sectional profile of the nanofiber.

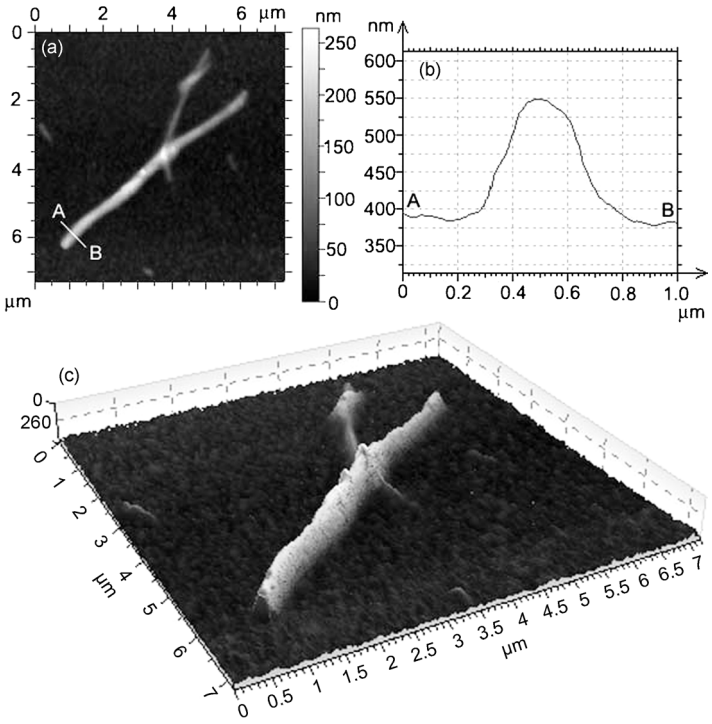

Figure 4. a) Tapping-mode AFM image, b) cross-sectional profile, and c) 3D profile of PTCz6 nanofibers on a glass substrate.

In these images, two fibers are crossed on the substrate. The length of the longer fiber was approximately 7 μm, and its diameter estimated from the cross-sectional profile was approximately 150 nm. This nanofiber was formed by self-aggregation during the electrochemical polymerization process. Furthermore, copolymers PTCz(5-7) and PTCz(4-8), which both have an average alkyl chain length of six, also show nanofiber formation (Figure 3i and j). However, polymer films prepared from TCz6 and TCz4 or TCz8 with different constituent ratios show that nanofiber formation in the resulting polymers disappears with deviation of the average alkyl chain length from six (Figures S4 and S5 in the Supporting Information). These results indicate that the chemical structures of monomers strongly affect the aggregation form of the resulting polymers. In this case, the relative proportion between flexible alkyl chain length and rigidity of the conjugated backbone is an important factor for nanofiber formation.

The entire series of PTCz*m* films shows the same UV/Vis–near infrared (NIR) absorption spectrum despite various alkyl chain lengths. Generally, conjugated polymer films prepared by electrochemical polymerization show no (or quite weak) fluorescence properties because of residual dopants (ions) in the films, well-aggregated structures of the polymers, and undesired crosslinks between conjugated main chains, which result in quenching of PL. Therefore, few papers have reported the PL and electroluminescence properties of electrosynthesized conjugated polymer films despite a large number of studies on electrosynthesized polymers.[38] However, the PTCz*m* films in this study show PL properties in their neutral state. Figure 5a and b show visual images of the PTCz6 film under irradiation by visible white light and UV light, respectively. Under white light, the neutral area (Figure 5a, left) of the polymer film appeared yellow, and the oxidized area (Figure 5a, right) appeared black. On the other hand, under incident UV light, the neutral area (Figure 5b, left) showed fluorescent light-green emission, whereas the oxidized area (Figure 5b, right) showed no emission. Absolute PL quantum yields of the polymer in the oxidized and neutral states are 0.32% (internal) and 0.30% (external), and 0.0035% (internal) and 0.0032% (external), respectively. The polymer in the neutral state exhibited an approximately 100 times higher value of the quantum yield than that of the polymer in the oxidized state. The difference in fluorescence intensity of the polymer between its oxidized and neutral states was also clearly observable by sight.

The PTCz6 film was also observed with a fluorescence microscope at 450–490 nm excitation wavelength (Figure 5c). On the neutral part, the PL emission from the nanofibers was observed, whereas on the oxidized part there was no PL emission. This quenching of the polymer film in the oxidized state is due to formation of radical cations (polarons) and dications (bipolarons) along the conjugated backbone generated by electrochemical oxidation.[39–41] In the neutral state, ground-state molecules are photoexcited by absorption of light at around 425 nm, which corresponds to the π–π* transition of the conjugated main chain. Then, the photoexcited molecules relax through a radiative pathway to emit green light ($\lambda_{em,max}=535$ nm; Figure S6 in the Supporting Information). In the oxidized state, nonradiative

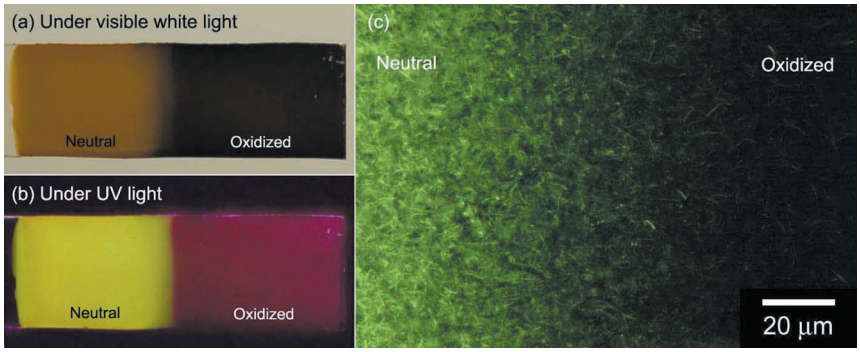

Figure 5. Photographs of PTCz6 nanofiber film deposited on an ITO glass electrode, which is half neutral (left) and half oxidized (right), a) under visible white light and b) under incident UV light. c) Fluorescence microscopy image of the surface of the PTCz6 film at the boundary between neutral (left) and oxidized (right) parts.

exciton decay occurs at polaronic quenching centers, thereby resulting in a depression of PL intensity.

The UV/Vis–NIR absorption and PL spectra of the PTCz6 film changed repeatedly during electrochemical redox processes. Figure 6 shows UV/Vis–NIR absorption spectra of PTCz6 film at various applied potentials with a three-electrode system. At −0.2 V (vs. Ag/Ag^+), in the reduced state, the polymer shows only an absorption band at 425 nm due to the π–π* transition of the conjugated main chains. The 425 nm absorption band decreased and blueshifted to 407 nm with an increase of the potential, and new absorption bands (doping bands) at around 565 and 1300 nm appeared, which correspond to polarons (radical cations) and bipolarons (dications), respectively, generated by the oxidation of the conjugated backbone. The blueshift of the π–π* transition band was observed due to shortening of the effective conjugation length of the main chain by polarons and bipolarons.[40] On the other hand, during the reduction process, the polaron and bipolaron bands disappeared and the 425 nm band regained its original intensity. Notably, a large optical change was observed at 0.4–0.5 V in the oxidation process, whereas a gradual change was observed during the reduction process. In other words, a nonlinear spectral change in the intensities was observed during the electrochemical process. Dyer et al. reported these phenomena for electrochromic poly(dialkoxythiophene)s,[13] and referred to a cooperative intramolecular domino effect, which is similar to the "twiston" described by Leclerc for the thermochromism of poly(alkylthiophene)s and poly(alkoxythiophene)s.[42]

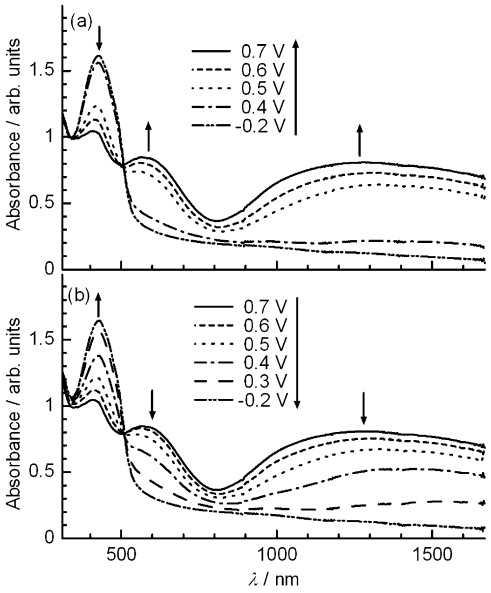

Figure 6. In situ UV/Vis–NIR spectra of PTCz6 deposited on an ITO glass electrode at various applied potentials (vs. Ag/Ag^+) during electrochemical a) oxidation and b) reduction processes (arb. = arbitrary).

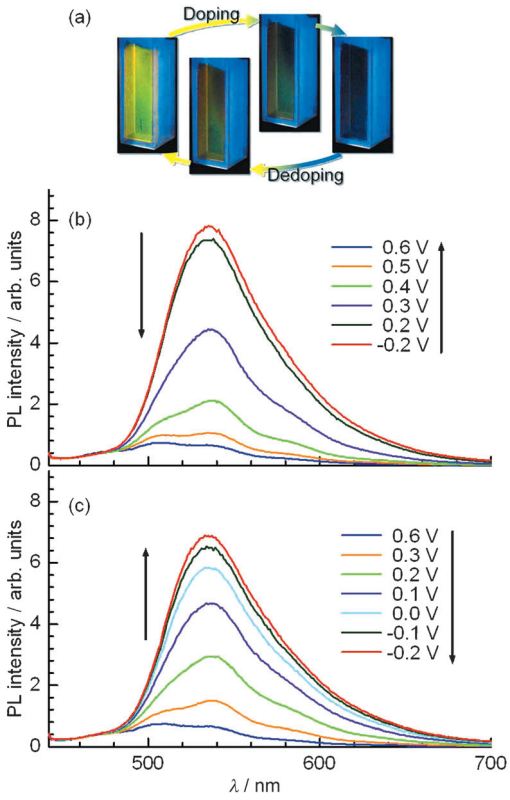

Figure 7. a) Visual images and b,c) in situ PL spectra of the PTCz6 deposited on an ITO glass electrode at various applied potentials (vs. Ag/Ag^+) during electrochemical b) oxidation and c) reduction processes.

Figure 7 shows the PL spectra of the PTCz6 film with an excitation wavelength of 425 nm at various applied potentials with a three-electrode system (vs. Ag/Ag^+). In the reduced state, the PTCz6 film emitted green light at 535 nm, the intensity of which declined with an increase in the applied potential. Then, in the oxidized state at 0.6 V (Ag/Ag^+), the polymer exhibited no PL because the formation of polarons and bipolarons in the conjugated main chain of the polymer promoted nonradiative decay rather than a radiative pathway for the energy relaxation of the photoexcited state. In the reduction process, the PL intensity was gradually recovered with a decrease in the applied potential.

To examine the repeatability of the electrochromic properties, the changes in absorption intensity at 425, 565, and 1300 nm and PL intensity at 535 nm of the PTCz6 film during repeated potential cycles were investigated (Figure 8). The potentials were applied sequentially between −0.2 and 0.6 V (vs. Ag/Ag^+) with a scan rate of 100 $mV\,s^{-1}$ for 400 s. The absorption and PL intensities responded to the periodic potential cycles. In the absorption intensity, the PTCz6 film showed good repeatability. After the first cycle, the PL intensity was restored to 90% of that from the initial stage. After the second cycle it showed approximately 99% repeatable restoration from the previous intensities. After 24 cycles, the reversibility slightly decreased to 82% of the initial intensity. These results demonstrate that the polymer

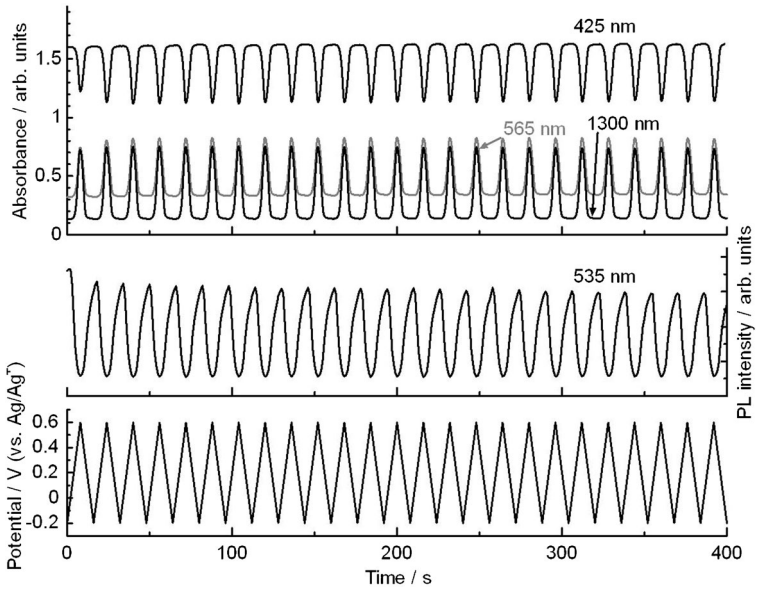

Figure 8. Time dependence of UV/Vis–NIR absorption intensity at 425, 565, and 1300 nm and PL intensity at 535 nm of PTCz6 film during repeated potential cycles. The potential was repeatedly applied between −0.2 and 0.6 V (vs. Ag/Ag^+) with a scan rate of 100 $mV\,s^{-1}$ for 400 s.

shows dynamically controllable change in emission with good repeatability. It is well known that the 3- and 6-positions of carbazole are reactive even after substitution or polymerization at the 2- and 7-positions. However, within the potential range up to 0.65 V (vs. Ag/Ag^+), PTCz6 exhibited a repeatable redox behavior even after 20 potential cycles unless a potential larger than 0.8 V (vs. Ag/Ag^+) was applied, which led to an unfavorable oxidative cross-linking reaction between the 3- and 6-positions of the carbazole units of adjacent polymer chains, thereby resulting in unrepeatable redox switching (Figure S8 in the Supporting Information).

Polarized PL emission from the PTCz6 nanofiber was observed visually by polarized fluorescence microscopy. Figure 9a and b show polarized fluorescence microscopy images of the PTCz6 nanofibers under incident UV light with different polarizer directions. In the polarizer direction perpendicular to the nanofiber, PL emission from the nanofiber was brighter than that in the parallel direction. This indicated that conjugated main chains of PTCz6 align perpendicular to the longitudinal axis of the nanofiber because linear conjugated polymers usually have transition dipole moments along the conjugated backbone. The molecular orientation in the nanofibers of this study was different from that of conjugated polymer nanofibers prepared by electrospinning, in which conjugated main chains were oriented along the longitudinal axis of the fibers.[33,43] The molecular orientation reported herein was similar to that of polythiophene nanofibers fabricated by using cast film, a whisker method, or shadow masks, in which the polymer chains were packed with their longitudinal axis perpendicular to the nanofiber axis.[31,44,45]

Furthermore, X-ray diffraction (XRD) measurements for the PTCz6 nanofiber film deposited on an ITO glass electrode were performed to examine the ordered structure of the polymer chains in the nanofibers. Figure 10 shows XRD patterns of the PTCz6 film and an ITO glass electrode substrate (the peak at 21.3° is due to a characteristic diffraction from the ITO glass electrode). The XRD pattern of the PTCz6 film shows well-defined peaks at around 2.7 and 4.4° ($=2\theta$), which correspond to 32.1 and 20.1 Å d spacings, respectively. These d spacings are in good agreement with theoretically calculated distances between adjacent alkyl chains perpendic-

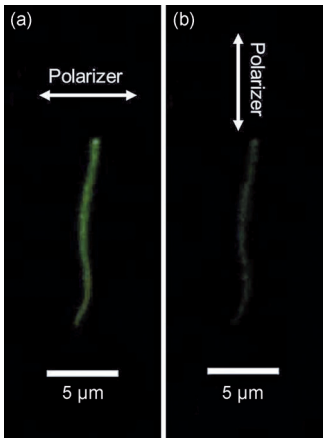

Figure 9. Polarized fluorescence microscopy images of a PTCz6 nanofiber with the polarizer direction a) perpendicular and b) parallel to a PTCz6 nanofiber.

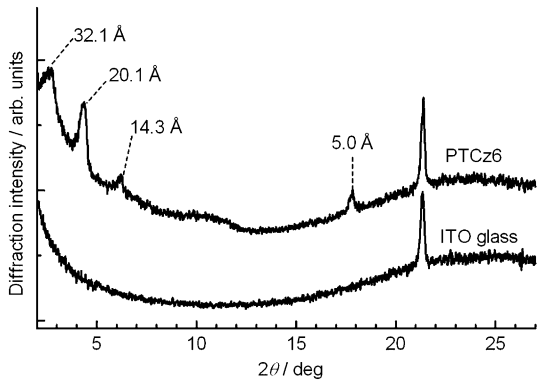

Figure 10. XRD patterns of PTCz6 nanofiber film deposited on an ITO glass electrode (top) and an uncoated ITO glass electrode (bottom).

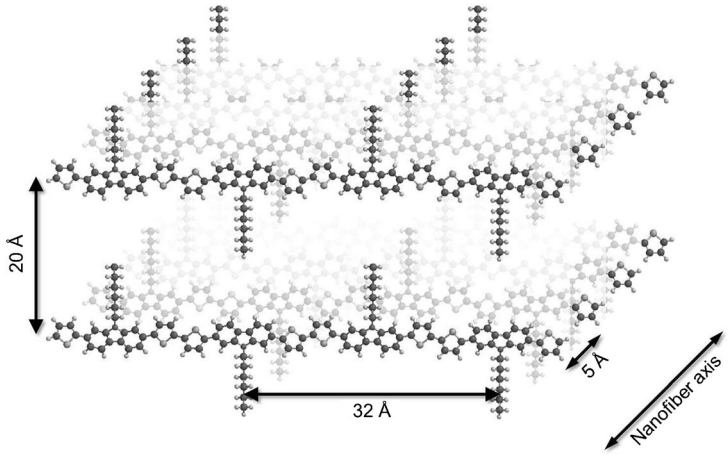

Figure 11. Schematic illustration of a possible packing structure of PTCz6 chains into nanofibers.

ular to the main chain, which are alternately substituted in opposite directions, and between adjacent main chains (Figure 11). The XRD pattern also shows two small peaks at 6.2 and 17.8° ($=2\theta$), which correspond to 14.3 and 5.0 Å *d* spacings, respectively. The 5.0 Å *d* spacing is assignable to the π-stacking distance between the main chains. These results lead to a possible structure of polymer chain packing of PTCz6 in the nanofiber, as shown in Figure 11. However, PTCz(5-7) and PTCz(4-8) nanofiber films show no such XRD pattern and polarized emission, thus indicating lower crystallinity in the form of the nanofibers. In electrochemical polymerization, the solubility of the growing polymer decreases as the polymerization reaction proceeds, which results in nucleation on the electrode followed by a solid-state polymerization reaction. The solubility of PTCz*m* depends on the alkyl chain length and the degree of polymerization, and the polymer has good intermolecular π–π interaction due to the good coplanarity and symmetry of carbazole and bithiophene units in the backbone. Therefore, aggregation occurs as a result of the competition between the solubility and intermolecular π–π interaction of the polymers, which determines the surface morphology. The competition can be a crucial factor for nanofiber formation of PTCz*m*. To date, many fluorescent conjugated polymer nanofibers have been reported, most of which are hybrid materials with organic polymer matrices or an inorganic template.[33,43,46] In contrast, the PTCz6 nanofiber is made purely from a conjugated polymer that has fluorescence and structural order, which can be applied to new optoelectronic devices.

Conclusion

Electrochemical polymerization of TCz*m* in acetonitrile was performed to afford electroactive fluorescent polymer films, the surface morphology of which strongly depends on the alkyl chain length. Among these polymers, PTCz6, PTCz(5-7), and PTCz(4-8) show nanofiber formation, which indicates that the proportion of the alkyl chain length relative to the conjugated backbone is important for nanofiber formation. The nanofibers thus prepared showed dynamically controllable electrofluorescence chromism. This could be applied to fluorescent-type passive indicator and display devices. Furthermore, PTCz6 nanofibers showed polarized emission, in which the polarizing direction was perpendicular to the fiber axis. XRD measurements of PTCz6 showed that the polymer chains possessed crystalline order in the nanofibers. This nontemplate bottom-up formation of nanofibers is due to self-assembly of growing polymers during electrochemical polymerization. Thus, electrochemical polymerization can be a straightforward method to deposit nanostructured polymers on electrode substrates under certain conditions and with appropriate molecular shape of the monomers, from the viewpoint of bottom-up technology.

Experimental Section

Materials: TCz*m* was synthesized according to the method reported previously.[34] The synthetic routes to the monomers are summarized in the Supporting Information.

Electrochemical polymerization: Electrochemical polymerization and copolymerization of TCz*m* were carried out by repeated potential cycling with a three-electrode system, which consisted of an indium tin oxide (ITO)-coated glass or platinum disk working electrode, an Ag/Ag^+ reference electrode, and a platinum wire counter electrode. The electrolyte solution consisted of tetrabutylammonium perchlorate (0.1 M) and monomers (1.0 mM) in acetonitrile. The scan rate was $100\,mV\,min^{-1}$. In the case of electrochemical copolymerization, the concentration of each monomer was 0.5 mM.

Acknowledgements

We would like to thank the Chemical Analysis Center of the University of Tsukuba and the Glass Workshop of the University of Tsukuba. K.K. is a research fellow of the Japan Society for the Promotion of Science. The research was supported by a Japan Society for the Promotion of Science (JSPS) Grant-in-Aid for Scientific Research (No. 22550161). We are grateful to JASCO Corporation for measurements of photoluminescence quantum yields of the polymer films.

[1] A. Loudet, K. Burgess, *Chem. Rev.* **2007**, *107*, 4891–4932.
[2] A. F. Mensinger, J. F. Case, *J. Exp. Mar. Biol. Ecol.* **1990**, *144*, 1–15.
[3] E. B. Namdas, P. Ledochowitsch, J. D. Yuen, D. Moses, A. J. Heeger, *Appl. Phys. Lett.* **2008**, *92*, 183304.
[4] A. Garcia, R. C. Bakus II, P. Zalar, C. V. Hoven, J. Z. Brzezinski, T. Q. Nguyen, *J. Am. Chem. Soc.* **2011**, *133*, 2492–2498.
[5] H. Nie, Y. Zhao, M. Zhang, Y. Ma, M. Baumgarten, K. Müllen, *Chem. Commun.* **2011**, *47*, 1234–1236.
[6] A. Bajaj, O. R. Miranda, R. Phillips, I. B. Kim, D. J. Jerry, U. H. F. Bunz, V. M. Rotello, *J. Am. Chem. Soc.* **2010**, *132*, 1018–1022.
[7] K. Wagner, R. Byrne, M. Zanoni, S. Gambhir, L. Dennany, R. Breukers, M. Higgins, P. Wagner, D. Diamond, G. G. Wallace, D. L. Officer, *J. Am. Chem. Soc.* **2011**, *133*, 5453–5462.
[8] J. Buey, T. M. Swager, *Angew. Chem.* **2000**, *112*, 622–626; *Angew. Chem. Int. Ed.* **2000**, *39*, 608–612.
[9] V. V. Roznyatovskiy, N. V. Roznyatovskaya, H. Weyrauch, K. Pinkwart, J. Tübke, J. L. Sessler, *J. Org. Chem.* **2010**, *75*, 8355–8362.
[10] H. B. Bu, G. Götz, E. Reinold, A. Vogt, S. Schmid, R. Blanco, J. L. Segura, P. Bäuerle, *Chem. Commun.* **2008**, 1320–1322.

[11] S. Sadki, P. Schottland, N. Brodie, G. Sabouraud, *Chem. Soc. Rev.* **2000**, *29*, 283–293.
[12] J. Roncali, *Chem. Rev.* **1992**, *92*, 711–738.
[13] A. L. Dyer, M. R. Craig, J. E. Babiarz, K. Kiyak, J. R. Reynolds, *Macromolecules* **2010**, *43*, 4460–4467.
[14] a) N. Akbaşoğlu, A. Balan, D. Baran, A. Cirpan, L. Toppare, *J. Polym. Sci. Part A Polym. Chem.* **2010**, *48*, 5603–5610; b) G. Sonmez, H. B. Sonmez, C. K. F. Shen, R. W. Jost, Y. Rubin, F. Wudl, *Macromolecules* **2005**, *38*, 669–675; c) M. İçli-Özkut, J. Mersini, A. M. Önal, A. Cihaner, *J. Polym. Sci. Part A Polym. Chem.* **2012**, *50*, 615–621; d) E. Sefer, F. B. Koyuncu, E. Oguzhan, S. Koyuncu, *J. Polym. Sci. Part A Polym. Chem.* **2010**, *48*, 4419–4427.
[15] Y. Lv, L. Yao, C. Gu, Y. Xu, D. Liu, D. Lu, Y. Ma, *Adv. Funct. Mater.* **2011**, *21*, 2896–2900.
[16] C. Gu, T. Fei, M. Zhang, C. Li, D. Lu, Y. Ma, *Electrochem. Commun.* **2010**, *12*, 553–556.
[17] a) C. Gu, T. Fei, L. Yao, Y. Lv, D. Lu, Y. Ma, *Adv. Mater.* **2011**, *23*, 527–530; b) C. Gu, T. Fei, Y. Lv, T. Feng, S. Xue, D. Lu, Y. Ma, *Adv. Mater.* **2010**, *22*, 2702–2705.
[18] E. Hwang, K. M. Nalin de Silva, C. B. Seevers, J. R. Li, J. C. Garno, E. E. Nesterov, *Langmuir* **2008**, *24*, 9700–9706.
[19] P. Kumar, K. Ranjith, S. Gupta, P. C. Ramamurthy, *Electrochim. Acta* **2011**, *56*, 8184–8191.
[20] D. A. Rider, K. D. Harris, D. Wang, J. Bruce, M. D. Fleischauer, R. T. Tucker, M. J. Brett, J. M. Buriak, *ACS Appl. Mater. Interfaces* **2009**, *1*, 279–288.
[21] T. Darmanin, F. Guittard, *J. Am. Chem. Soc.* **2011**, *133*, 15627–15634.
[22] A. Ashrafi, M. A. Golozar, S. Mallakpour, *Synth. Met.* **2006**, *156*, 1280–1285.
[23] L. Niua, C. Kvarnströma, K. Fröberg, A. Ivaska, *Synth. Met.* **2001**, *122*, 425–429.
[24] L. Liang, J. Liu, C. F. Windisch, G. J. Exarhos, Y. Lin, *Angew. Chem.* **2002**, *114*, 3817–3820; *Angew. Chem. Int. Ed.* **2002**, *41*, 3665–3668.
[25] C. R. Martin, *Acc. Chem. Res.* **1995**, *28*, 61–68.
[26] C. Li, H. Bai, G. Shi, *Chem. Soc. Rev.* **2009**, *38*, 2397–2409.
[27] M. Li, Z. Wei, L. Jiang, *J. Mater. Chem.* **2008**, *18*, 2276–2280.
[28] D. Li, J. Huang, R. B. Kaner, *Acc. Chem. Res.* **2009**, *42*, 135–145.
[29] S. Y. Jang, V. Seshadri, M. S. Khil, A. Kumar, M. Marquez, P. Mather, G. Sotzing, *Adv. Mater.* **2005**, *17*, 2177–2180.
[30] J. D. Fowler, S. Virji, R. B. Kaner, B. H. Weiller, *J. Phys. Chem. C* **2009**, *113*, 6444–6449.
[31] J. A. Merlo, C. D. Frisbie, *J. Phys. Chem. B* **2004**, *108*, 19169–19179.
[32] X. Li, S. Tian, Y. Ping, D. H. Kim, W. Knoll, *Langmuir* **2005**, *21*, 9393–9397.
[33] D. Tu, S. Pagliara, A. Camposeo, L. Persano, R. Cingolani, D. Pisignano, *Nanoscale* **2010**, *2*, 2217–2222.
[34] K. Kawabata, H. Goto, *Synth. Met.* **2010**, *160*, 2290–2298.
[35] J. Doskocz, M. Doskocz, S. Roszak, J. Soloducho, J. Leszczynski, *J. Phys. Chem. A* **2006**, *110*, 13989–13994.
[36] J. Casado, S. Hotta, V. Hernández, J. T. L. Navarrete, *J. Phys. Chem. A* **1999**, *103*, 816–822.
[37] J. Casado, H. E. Katz, V. Hernández, J. T. L. Navarrete, *Vib. Spectrosc.* **2002**, *30*, 175–189.
[38] a) X. Sun, Y. Liu, S. Chen, W. Qiu, G. Yu, Y. Ma, T, Qi, H. Zhang, X. Xu, D. Zhu, *Adv. Funct. Mater.* **2006**, *16*, 917–925; b) J. Xu, G. Shi, J. Zhang, X. Hong, *Macromol. Chem. Phys.* **2002**, *203*, 2385–2390; c) G. Casalbore-Miceli, N. Camaioni, V. Fattori, A. M. Fichera, M. C. Gallazzi, A. Geri, E. Girotto, G. Giro, *Synth. Met.* **2001**, *121*, 1575–1576.
[39] K. Kaneto, S. Hayashi, K. Yoshino, *J. Phys. Soc. Jpn.* **1988**, *57*, 1119–1126.
[40] S. Hayashi, K. Kaneto, K. Yoshino, *Solid State Commun.* **1987**, *61*, 249–251.
[41] D. D. C. Bradley, R. H. Friend, *J. Phys. Condens. Matter* **1989**, *1*, 3671–3678.
[42] M. Leclerc, *Adv. Mater.* **1999**, *11*, 1491–1498.
[43] S. Pagliara, M. S. Vitiello, A. Camposeo, A. Polini, R. Cingolani, *J. Phys. Chem. C* **2011**, *115*, 20399–20405.
[44] a) S. Samitsu, T. Shimomura, S. Heike, T. Hashizume, K. Ito, *Macromolecules* **2008**, *41*, 8000–8010; b) T. Shimomura, T. Takahashi, Y, Ichimura, S. Nakagawa, K. Noguchi, S. Heike, T. Hashizume, *Phys. Rev. B* **2011**, *83*, 115314.
[45] R. Zhang, B. Li, M. C. Iovu, M. Jeffries-EL, G. Sauvé, J. Cooper, S. Jia, S. Tristram-Nagle, D. M. Smilgies, D. N. Lambeth, R. D. McCullough, T. Kowalewski, *J. Am. Chem. Soc.* **2006**, *128*, 3480–3481.
[46] N. Jiravanichanun, K. Yamamoto, A. Irie, H. Otsuka, A. Takahara, *Synth. Met.* **2009**, *159*, 885–888.

Received: April 28, 2012
Revised: August 9, 2012
Published online: October 2, 2012

